Liquid Crystals
Publication details, including instructions for authors and subscription information:
http://www.informaworld.com/smpp/title~content=t713926090

Cholesteric blue phases: effect of strong confinement

J. Fukuda[ab]; S. Žumer[bc]
[a] Nanotechnology Research Institute, National Institute of Advanced Industrial Science and Technology (AIST), 1-1-1, Umezono, Tsukuba, Japan [b] Department of Physics, University of Ljubljana, Ljubljana, Slovenia [c] Jožef Stefan Institute, Ljubljana, Slovenia

Online publication date: 06 July 2010

To cite this Article Fukuda, J. and Žumer, S.(2010) 'Cholesteric blue phases: effect of strong confinement', Liquid Crystals, 37: 6, 875 — 882
To link to this Article: DOI: 10.1080/02678292.2010.481909
URL: http://dx.doi.org/10.1080/02678292.2010.481909

Liquid Crystals,
Vol. 37, Nos. 6–7, June–July 2010, 875–882

Taylor & Francis
Taylor & Francis Group

INVITED ARTICLE

Cholesteric blue phases: effect of strong confinement

J. Fukuda[a,b*] and S. Žumer[bc]

[a]*Nanotechnology Research Institute, National Institute of Advanced Industrial Science and Technology (AIST), 1-1-1 Umezono, Tsukuba 305-8568, Japan;* [b]*Department of Physics, University of Ljubljana, Jadranska 19, 1000 Ljubljana, Slovenia;* [c]*Jožef Stefan Institute, Jamova 39, 1000 Ljubljana, Slovenia*

(*Received 3 February 2010; accepted 17 March 2010*)

After an overview of cholesteric blue phases, we review our recent numerical studies on possible defect structures when blue phase I (BP I) is confined in a thin cell composed of two parallel surfaces imposing homeotropic anchoring. The cell thickness is of the order of the unit cell dimension of the bulk cubic BP I. We find several structures of disclination lines which, to our knowledge, have never been discussed in the field of liquid crystals as equilibrium structures. Those structures include a parallel array of double helix disclination lines, and two parallel arrays of undulating disclination lines almost (but not exactly) perpendicular to each other. A first-order transition between those two structures is possible, and the similarity between them is discussed.

Keywords: cholesteric blue phase; confinement; Landau–de Gennes theory; disclination; double-helix structures

1. Introduction

Cholesteric blue phases (BPs) [1–8] are peculiar chiral mesophases that occur over a narrow temperature range between the isotropic and cholesteric, or chiral nematic, phases of highly chiral compounds. Blue phases provide an intriguing example of a three-dimensional ordered structure of a liquid crystal, and an important key to the understanding of the structures is that a local double-twist structure, in which the directors display helical ordering along two orthogonal directions, is energetically preferred in comparison to a simple-twist cholesteric structure. Double-twist order is perfectly realised in the centre of a cylinder, while with increased radius it is less and less pronounced. This leads to a limitation on the double-twist cylinder diameter and thus to phases with spatial superstructures of double-twist cylinders. Due to topological constraints on the nematic ordering, the arrangement of double-twist cylinders is complemented by a network of disclination lines with $-1/2$ winding number. The structure can be understood in terms of a delicate balance between energetically favourable regions of double-twist order and the energetic cost of disclination lines. These complex structures yield phases with an effective isotropic index of refraction (no birefringence) but with high rotary power of polarised light.

Alfred Saupe [9] was the first to recognise that cubic symmetry of the twisted director field accompanied with a network of disclinations is needed to describe a blue phase with optical isotropy. He proposed a model based on minimal periodic surfaces forming a cubic lattice with O^5 ($I432$) symmetry [9]. Later, detailed experimental studies, reviewed in depth in [2, 5, 6, 8], showed that Saupe's BP model is not realised in nature where three thermodynamically distinct blue phases can be observed. Depending on the strength of the molecular chirality they occur in the order BP III, BP II, BP I upon lowering the temperature. The BP III has an amorphous assembly of double-twist forms with the same symmetry as the isotropic fluid. In contrast, BP I and BP II both exhibit orientational order on a cubic lattice with unit cells of several hundred nanometres, thus leading to Bragg reflection of light in the visible and ultraviolet wavelength range. The corresponding space groups are O^{8-} ($I4_132$) and $O^2(P4_232)$, respectively, and illustrations of the structures of BP I and II are given in Figure 1.

The unique combination of full fluidity and three-dimensional crystalline orientational order makes the cubic blue phases highly appealing for optical applications. Unfortunately, the delicate balance between the formation of double-twist and disclination lines yields a narrow stability range of the blue phases. Typically, the range is less than 1 K just below the isotropic phase and thus providing severe limitations to any potential device application. However, recently blue phases with substantially extended stability ranges, of more than 40 K including room temperature, have been reported in systems using the photo-crosslinking of polymers [10] or the addition of bimesogenic units [11]. Realisation of blue phases with a wide temperature

*Corresponding author. Email: fukuda.jun-ichi@aist.go.jp

ISSN 0267-8292 print/ISSN 1366-5855 online

DOI: 10.1080/02678292.2010.481909
http://www.informaworld.com

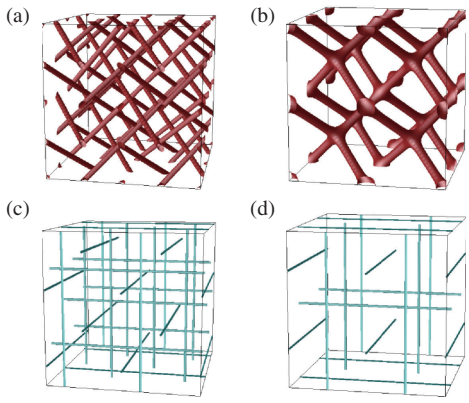

Figure 1. Illustrations of the configuration of disclination lines of (a) blue phase I (BP I) and (b) blue phase II (BP II). Also shown are schematic illustrations of the arrangement of double-twist cylinders in (c) BP I and (d) BP II. In each figure, $2 \times 2 \times 2$ unit cells are shown. Note that the size of these figures does not reflect the actual dimension of the unit cell (that of BP I is larger than that of BP II).

range has revived interest in the possibility of practical application of blue phases. Lasing of blue phases was reported [12, 13] and recently also the first display based on the switching of the blue phase structure was constructed [14].

Theoretical studies to understand the structures of blue phases were carried out mainly in the 1980s following on from insight of Saupe [9] on their cubic nature and the accumulation of experimental knowledge. Although some are based on a Frank elastic theory in terms of a director $\boldsymbol{n}$ [15, 16], many of them deal with the orientational order using a second-rank tensor order parameter $Q_{\alpha\beta}$ following in the spirit of Landau and de Gennes [3, 17, 18] (and references therein). Those analytical studies contributed greatly to the clarification of the equilibrium properties of cubic blue phases. However, it was not clear whether mode expansions of $Q_{\alpha\beta}$ necessary for the calculations to be analytically tractable were fully justified. Since 2005, there have been several numerical attempts [19–26] to evaluate the order parameter profile of blue phases without relying on mode expansions. Those studies concern phase diagrams [19, 20], structural changes under an applied electric field [21, 24], and blue phases with colloidal particles [26].

In the present paper, we review our recent study on the effect of strong confinement on the defect structures of cholesteric blue phases, which was presented briefly in our previous letter [25]. Although a liquid crystal in confined geometries is an important subject in practical applications such as liquid crystal displays, as well as in fundamental science [27], only very few studies, which are interested in blue phases in the Cano-wedge geometry [28, 29], have been carried out to investigate how blue phases behave in confinement. Here we are interested in the configurations of cholesteric blue phases in a thin planar cell where the separation of the two surfaces is of the order of the dimension of the bulk BP unit cell. We will show in detail the defect structures found in our numerical calculations.

2. Theoretical modelling for confined blue phases

2.1 Landau–de Gennes theory for chiral liquid crystals

In a Landau–de Gennes theory of a nematic liquid crystal, the orientational order of a liquid crystal is described by a symmetric and traceless second-rank tensor $Q_{\alpha\beta}$, instead of a director $\boldsymbol{n}$ commonly used in a Frank elastic theory. One of the great advantages of the Landau–de Gennes theory is that topological defects such as disclination lines need not be treated as singularities, which facilitates greatly the investigation of problems concerning topological defects, especially when we want to tackle them numerically.

Now we write down the free energy density of a bulk liquid crystal in terms of the order parameter $Q_{\alpha\beta}$. The local part of the free energy density f_{local} is given by a Landau expansion, and terms up to fourth order are retained in many practical problems (say, the nematic–isotropic transition, although the description of biaxial nematics requires higher order terms). Then f_{local} reads

$$f_{\mathrm{local}} = c\,\mathrm{TrQ}^2 - \sqrt{6}b\,\mathrm{TrQ}^3 + a(\mathrm{TrQ}^2)^2, \qquad (1)$$

where $\mathrm{TrQ}^2 = \mathrm{Q}_{\alpha\beta}\mathrm{Q}_{\alpha\beta}$ and $\mathrm{TrQ}^3 = \mathrm{Q}_{\alpha\beta}\mathrm{Q}_{\beta\gamma}\mathrm{Q}_{\gamma\alpha}$ (here and in the following, summations over repeated indices are implied). The parameters a, b and c depend on the material and the temperature, and a must be positive for f_{local} to be positive definite. In the usual treatment of a Landau theory, only the parameter c is regarded as temperature dependent (linear in relative or shifted temperature); the temperature dependence of the other parameters is assumed to play no significant role.

The elastic energy taking care of the spatial variation of the orientational order can be taken into account by collecting scalar terms allowed by symmetry that are constructed from $Q_{\alpha\beta}$ and the gradients ∂_γ. In the case of an achiral nematic possessing rotational symmetry and inversion symmetry, $\partial_\gamma Q_{\alpha\beta}\partial_\gamma Q_{\alpha\beta}$ and $\partial_\beta Q_{\alpha\beta}\partial_\gamma Q_{\gamma\alpha}$ must be retained when we are interested in terms up to second order in the gradients and in $Q_{\alpha\beta}$. Another term allowed by symmetry, $\partial_\gamma Q_{\alpha\beta}\partial_\beta Q_{\gamma\alpha}$, is converted to $\partial_\beta Q_{\alpha\beta}\partial_\gamma Q_{\gamma\alpha}$ plus a divergent term that can be converted to a surface integral, $\partial_\gamma(Q_{\alpha\beta}\partial_\beta Q_{\gamma\alpha} - Q_{\alpha\gamma}\partial_\beta Q_{\beta\alpha})$. To the best of our knowledge, in previous literature on the Landau–de Gennes

theory, the effect of the latter divergent term has neither been discussed theoretically nor experimentally, because it is irrelevant in an infinite system, or in the case of the strong anchoring limit. However, it can play some role in the following problem concerning a liquid crystal in contact with confining surfaces. In the present study we ignore it for simplicity and do not discuss its possible role. In the case of a chiral liquid crystal with no inversion symmetry, an additional term that is first order in the gradient, i.e. $Q_{\alpha\beta}(\nabla \times Q)_{\alpha\beta} \equiv Q_{\alpha\beta}\epsilon_{\alpha\gamma\delta}\partial_\gamma Q_{\delta\beta}$ is possible (here $\epsilon_{\alpha\gamma\delta}$ is the Levi-Civita antisymmetric symbol). Collecting the three terms we have mentioned, the elastic energy density of a (chiral) nematic liquid crystal is written as

$$f_{\rm el}\{Q_{\alpha\beta}, \nabla\} = \frac{1}{4}K_1[(\nabla \times Q)_{\alpha\beta} + 2q_0 Q_{\alpha\beta}]^2 + \frac{1}{4}K_0[(\nabla \cdot Q)_\alpha]^2, \quad (2)$$

where $(\nabla \cdot Q)_\alpha \equiv \partial_\beta Q_{\alpha\beta}$, K_0 and K_1 are the elastic constants, and $2\pi/|q_0|$ is the pitch of the cholesteric helix. We can also say that q_0 characterises the strength and sign of the chirality ($q_0 = 0$ for an achiral nematic). Note that the zeroth-order term in the gradients, $K_1 q_0^2 \mathrm{TrQ}^2$, can be absorbed in $f_{\rm local}$. We also note that in Equations (1) and (2) we have followed the notation of material parameters from Wright and Mermin [5], in contrast to the elastic constant L usually used in Landau–de Gennes theory. Furthermore, it should be stressed that the elastic constants in Equation (2) should not be confused with those in the original Frank theory of elasticity in terms of $\boldsymbol{n}$.

To study the effects of anchoring we choose the simplest geometry: an infinite thin film confined to a planar cell where two surfaces are separated by a distance d. Anchoring of a liquid crystal by confining surfaces is taken into account in a phenomenological manner by considering the surface free energy density in terms of $Q_{\alpha\beta}$. Here we discuss the cases with homeotropic anchoring, and employ the form of the surface anchoring energy first argued by Nobili and Durand [30]. The surface free energy density is then written as

$$f_{\rm s} = \frac{1}{2}W\,\mathrm{Tr}(\mathrm{Q} - \mathrm{Q_s})^2. \quad (3)$$

Here $(Q_{\rm s})_{\alpha\beta} = Q_0(\nu_\alpha\nu_\beta - (1/3)\delta_{\alpha\beta})$ defines the order parameter preferred by the surface, with Q_0 being the degree of orientational order. To mimic homeotropic anchoring, a unit vector ν must be taken along the surface normal. The total free energy of the system is written as

$$F_{\rm tot} = \int_\Omega dr^3\,(f_{\rm local} + f_{\rm el}) + \int_S dr^2 f_s, \quad (4)$$

where Ω is the volume occupied by the liquid crystal and S denotes the confining surfaces.

Equations (1)–(3) contain many material parameters, and their appropriate rescaling reduces the number of relevant parameters and can clarify the following discussions. For the bulk free energy densities $f_{\rm local}$ and $f_{\rm el}$, we employ the rescaling by Wright and Mermin [5] and introduce dimensionless quantities: the rescaled free energy densities

$$\varphi_{\rm local,el} \equiv (a^3/b^4) f_{\rm local,el} \quad (5)$$

and the rescaled order parameter

$$\chi_{\alpha\beta} \equiv (a/b) Q_{\alpha\beta}. \quad (6)$$

We note here that the rescaled order parameter can exceed unity. We measure lengths in units of $(2q_0)^{-1}$ and the rescaled gradient reads $\bar{\nabla} = (2q_0)^{-1}\nabla$. Then $\varphi_{\rm local}$ and $\varphi_{\rm el}$ are given by

$$\varphi_{\rm local}\{\chi_{\alpha\beta}\bar{\nabla}\} = \tau\,\mathrm{Tr}\boldsymbol{\chi}^2 - \sqrt{6}\,\mathrm{Tr}\boldsymbol{\chi}^3 + (\mathrm{Tr}\boldsymbol{\chi}^2)^2 \quad (7)$$

and

$$\varphi_{\rm el}\{\chi_{\alpha\beta}, \bar{\nabla}\} = \kappa^2\{[(\bar{\nabla} \times \chi)_{\alpha\beta} + \chi_{\alpha\beta}]^2 + \eta[(\bar{\nabla} \cdot \chi)_\alpha]^2\}. \quad (8)$$

Here $\tau \equiv (a/b^2)c$ is a rescaled relative temperature, and $\kappa \equiv \sqrt{aK_1 q_0^2/b^2}$ is a rescaled chirality. The parameter $\eta \equiv K_0/K_1$ concerns the anisotropy of the elasticity, and hereafter just for simplicity we set $\eta = 1$ (i.e. the one-constant approximation).

We rescale $f_{\rm s}$ so that the rescaled total free energy reads

$$\bar{F}_{\rm tot} \equiv (2q_0)^3(b^4/a^3)F_{\rm tot} = \int_\Omega d\bar{r}^3\,(\varphi_{\rm local} + \varphi_{\rm el}) + \int_S d\bar{r}^2\,\varphi_s, \quad (9)$$

with $\bar{\boldsymbol{r}} \equiv 2q_0\boldsymbol{r}$ being the rescaled length. The rescaled surface free energy density φ_s then reads

$$\varphi_{\rm s} = \frac{1}{2}w\,\mathrm{Tr}(\boldsymbol{\chi} - \boldsymbol{\chi}_{\rm s})^2, \quad (10)$$

with the rescaled anchoring strength $w = 2q_0(a/b^2)W$.

We conclude this subsection by commenting on the relevant parameters. Reliable material parameters in the Landau–de Gennes theory for liquid crystals showing blue phases are unfortunately unavailable (in particular a and b). However, from typical values

for an achiral nematic liquid crystal in [31, 32], we have $a \simeq 8 \times 10^4$ J m^{-3} and $b \simeq 5 \times 10^4$ J m^{-3}. Typical values of other parameters are $K_1 \simeq 10$ pN, $q_0 \simeq 4 \times 10^7$ m^{-1}. They yield $\kappa \simeq 0.7$, which we will employ in the following numerical calculations. For the rescaled temperature, we choose $\tau = -1$. We have confirmed in a previous calculation [24] that BP I is the most stable phase in the bulk with this choice of τ. We set the rescaled anchoring strength to $w = 0.5$, corresponding to an experimentally accessible value $W = 4 \times 10^{-4}$ J m^{-2}. This choice of w yields the extrapolation length $\xi_w \simeq 25$ nm (or $\simeq 2$ in units of $(2q_0)^{-1}$). As we will mention later, we are interested in the cases with the cell thickness of the order of 10 in units of $(2q_0)^{-1}$, and therefore $w = 0.5$ does not result in perfect homeotropic alignment at the surfaces. We note that the variation of w can significantly influence the stable structure as discussed in [25]; weaker anchoring with smaller w results in a structure similar to that of bulk blue phases in most cases, in contrast to the results presented later. As $\boldsymbol{\chi}_s$ in Equation (10), we choose $\chi_{s\alpha\beta} = \chi_{s0}(\nu_\alpha\nu_\beta - (1/3)\delta_{\alpha\beta})$ with $\boldsymbol{\chi}_{s0} = 1.44$, which corresponds to the order parameter that minimises the local free energy in Equation (7). In the following, all the variables and parameters are given in a rescaled form.

2.2 *Calculation of equilibrium structures*

As mentioned previously, we consider a liquid crystal confined in a cell made up of two parallel flat surfaces with a separation d. In the present calculations, the range of d is set to $9 \leq d \leq 18$, while the dimension of a unit cell of bulk BP I is 12.60. Therefore, we are interested in the region in which the cell thickness d is of the order of the dimension of bulk BP I.

We take the z-axis perpendicular to the confining surfaces, and discretise our system using a $32 \times 32 \times 33$ parallelepiped lattice, with periodic boundary conditions along the surfaces (i.e. the x and y directions). We relax the order parameter by a simple equation with rotational diffusion

$$(\partial/\partial t)\chi_{\alpha\beta}(\bar{\mathbf{r}}) = -\left(\delta\bar{F}_{\mathrm{tot}}/\delta\chi_{\alpha\beta}(\bar{\mathbf{r}}) - \lambda\delta_{\alpha\beta}(\bar{\mathbf{r}})\right),$$

where the time t is again appropriately rescaled. We also let the shape and size of the system in the x and y directions change according to the procedures presented in [24], while in the z direction the cell thickness d is fixed. By relaxing $\boldsymbol{\chi}$ and the shape of the system, we find the stable or metastable structures which give a (local) minimum of $\bar{F}_{\mathrm{tot}}$. As the initial condition, we employ the stable structure of bulk BP I for $\tau = -1$, $\kappa = 0.7$ and $\eta = 1$ obtained in [24], which is dilated or compressed along the z direction to conform to the thickness d of the system. As shown later, we can obtain various structures depending on d, and to check if those structures can exist in different d, we also perform calculations employing those structures as initial conditions.

3. Results

In Figures 2–4, we show some equilibrium structures found by our calculations (as briefly described in our letter [25] which do not resemble that of the blue phases in the bulk. In those figures, we focus on the configurations of topological disclination lines whose locations are highlighted. We discuss later the profiles of the orientational order for the former two structures in Figures 2 and 3.

We can see in Figure 2 disclination lines interwoven in a double-helical fashion, and those double-helices are located parallel with each other. In Figure 3, two parallel arrays of undulating disclination lines are arranged almost perpendicular to each other (although, as we will see later, they are not in fact perpendicular). Each array is located so that a set of disclination lines forms an undulating curved plane parallel to the confining

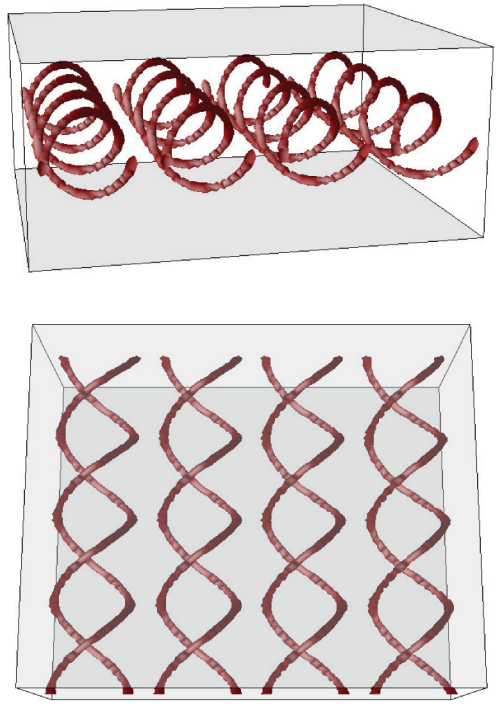

Figure 2. Visualisation of topological defects in a double-helix configuration. Side view (top) and top view (bottom). The confining surfaces are shown as grey planes. We show here 2×2 unit cells connected by periodic boundaries. The cell thickness, d, is 15.

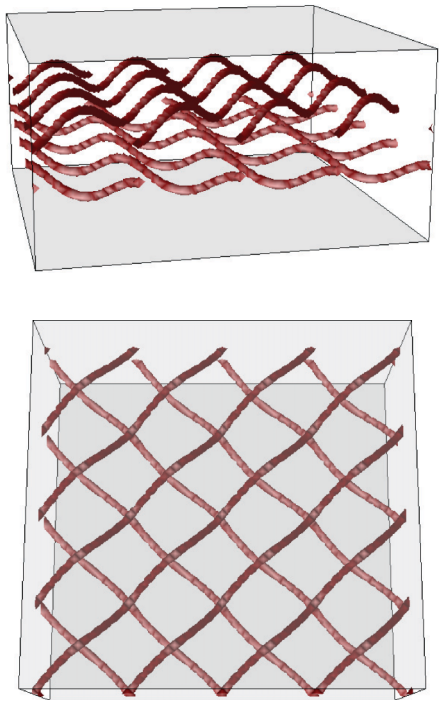

Figure 3. Visualisation of topological defects in a parallel-array configuration. The cell thickness, d, is 15.

surfaces. We also find a staggered structure of disclination lines in contact with the confining surfaces and shown in Figure 4. Disclination lines in contact with one confining surface look like inchworms, and align

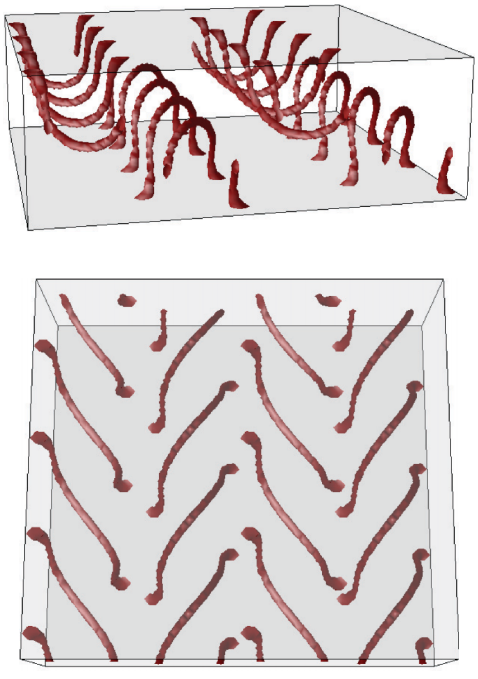

Figure 4. Visualisation of topological defects in a staggered configuration. The cell thickness, d, is 11.

parallel to each other. While in the bulk cubic blue phases the disclination lines are (at least locally) straight, in the presence of confining surfaces they have become curved. As we will see later, the structures in Figures 2 and 3 have several features in common; one is that the disclination lines do not touch the confining surfaces. Although Alexander and Marenduzzo [21] have reported structures of disclination lines similar to those found in Figures 2 and 3, they are transient states found when a strong electric field is applied to bulk blue phase II. As far as we know, those three structures in Figures 2–4 have never been observed in experiments, or discussed in theoretical or numerical studies as possible stable states of a liquid crystal.

In Figure 5, we show the thickness dependence of the total free energy of the system per unit area, $\mathcal{F} = (\bar{F}_{\rm tot} - f_0 d)/A$, with f_0 and A being the free energy density of bulk BP I and the area of one confining surface, respectively. For comparison, we also present the energies of the equilibrium structures similar to that of bulk BP I, and of a cholesteric phase in a uniform lying helix (ULH) configuration with the helical axis parallel to the confining surfaces. Note that the ULH configuration is energetically more favourable than the Grandjean configuration whose helical axis is along the surface normal; the latter is incompatible with the homeotropic alignment at the surfaces. The isotropic phase is unstable in the bulk in the present case with $\tau = -1$, and does not appear as a (meta)stable state in our system. We find that the double-helix configuration presented in Figure 2 is indeed stable in the range $10 \lesssim d \lesssim 14$. For $d \gtrsim 14$, the most stable structure is the parallel-array configuration shown in Figure 3. From Figure 5, a first-order transition between those two structures is expected and hysteresis can exist with the variation of d. The transition could also be induced by a change of temperature, although we have not yet investigated this possibility. The staggered structure shown in Figure 4 can be found to be the most stable one only in a very narrow range around $d \simeq 10$. At least in the range we study here, structures similar to the bulk BP I are found to be the energetically most favourable structure. This is possibly due to the energetic penalty of disclination lines in contact with confining surfaces with homeotropic anchoring; around disclination lines found in bulk blue phases (wedge disclinations of topological charge $-1/2$), the director tends to be parallel to the plane whose normal is along the disclination. This orientational order is incompatible with the homeotropic alignment at the confining surface when the disclinations touch the surface. We also notice that the structures in Figures 2 and 3 act as a harmonic spring in contrast to the cholesteric ULH

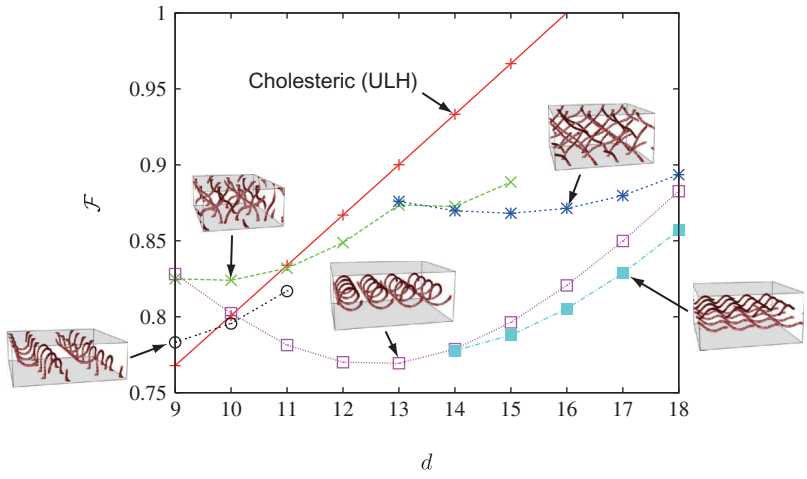

Figure 5. Variation of the free energy $\mathcal{F}$ with the cell thickness d. In addition to $\mathcal{F}$ for the structures shown in Figures 2–4, we also show $\mathcal{F}$ for the structures similar to bulk BP I ($\times$ and $*$), and for a cholesteric phase with a uniform lying helix (ULH) configuration.

state which would yield an attraction between confining surfaces almost independent of the cell thickness.

Here we discuss the similarity between the double-helix and the parallel-array configurations by showing their respective orientation profiles in Figures 6 and 7. We can find that the orientation profiles labelled by xz and yz are almost indistinguishable between those two profiles and the difference can only be seen in the profiles xy; disclination lines do not cross the plane (mid-plane of the cell) in the parallel-array configuration. The arrangement of double-twist cylinders is again almost the same for those two configurations. The similarity can also be recognised in the bottom figures of Figures 2 and 3. That is, the reconnection of disclination lines at the points where two lines come close can change one profile into the other. This inspection can explain qualitatively why the double-helix configuration is energetically preferred over the parallel-array configuration when d is relatively small. For smaller d in the parallel-array configuration, two almost-orthogonal disclination lines come closer and experience a strong repulsion from each other. However, once the reconnection occurs and the parallel-array configuration is transformed into the double-helix one, the disclination lines no longer feel the repulsion from the others. As mentioned previously, the transition between the two structures should be first order, and, therefore, their coexistence is possible at the transition point. We could also speculate that thermal fluctuations might result in a mixed configuration of double-twist and parallel-array close to the transition. We finally note that the two perpendicular directions along the confining surfaces (x and y) are no longer equivalent as is obvious from Figures 6 and 7, in contrast to the bulk blue phases I and II possessing

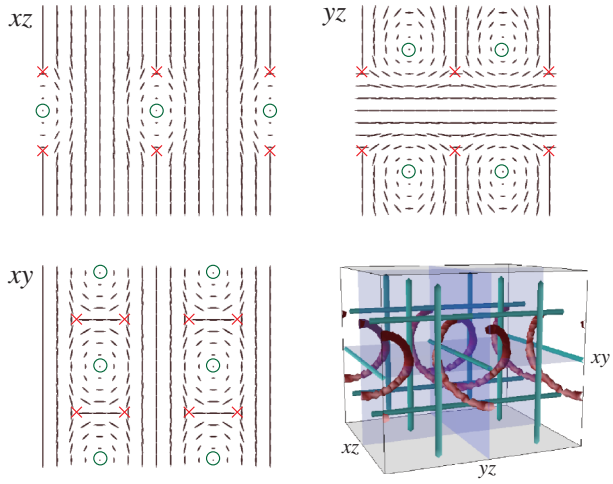

Figure 6. Orientation profiles of the double-helix structure in Figure 2 at the three cross sections (the location of the cross sections can be found in the right-hand bottom figure). Disclination lines and the axes of double-twist cylinders are shown by crosses ($\times$) and open circles ($\circ$), respectively. In the right-hand bottom figure, the arrangement of double-twist cylinders with respect to the disclination lines is illustrated schematically by thin straight cylinders.

cubic symmetry. Therefore, the two parallel arrays of apparently perpendicular disclination lines as shown in Figure 3 are in fact not orthogonal.

4. Conclusion

By using a numerical calculation based on a Landau–de Gennes theory describing the orientational order of a liquid crystal by a tensor order parameter, we have investigated the defect structures for a chiral liquid crystal under a strong confinement between two parallel flat surfaces. We have shown

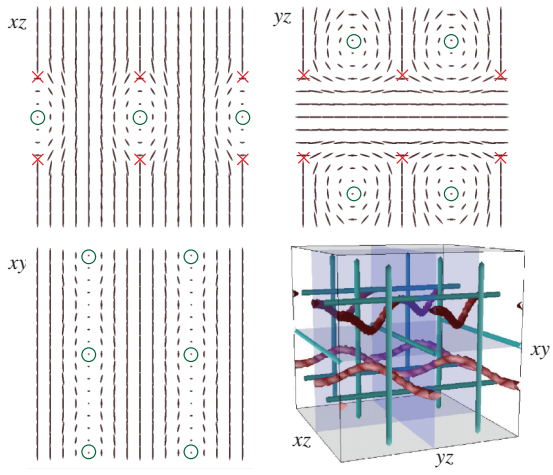

Figure 7. As Figure 6 for the parallel-array configuration shown in Figure 3.

the possibility of various defect structures not found nor discussed previously in the liquid crystal field as stable structures. For example, we have found a parallel array of double-helix disclinations, a set of two arrays of parallel undulating disclinations and a staggered structure of disclinations in contact with the confining surfaces. We have calculated the free energy of these structures and demonstrated that the former two can indeed be stable when the cell thickness is of the order of the dimension of the unit cell of the bulk blue phases. We have discussed the similarity between those two configurations and pointed out the possibility of first-order phase transition.

Experimental verification of these possible structures is strongly encouraged, and much remains to be investigated in the behaviour of cholesteric blue phases under strong confinement, for instance, the effect of temperature change, anchoring conditions (say, planar anchoring) or the type of confinement (cylindrical capillary etc.). Nevertheless, we believe that we have shown an important and intriguing example of frustrations between the self-organised structure of a (bulk) liquid crystal and the external condition imposed by confinement. We further note the similarities between blue phases and other systems. It has been argued theoretically [33–35] that chiral ferromagnets such as MnSi can have ordered structures analogous to blue phases. Topological excitations called Skyrmions, of which double-twist cylinders are a typical example, have been known to exist in a wide variety of physical systems such as spinor Bose–Einstein condensates [36], and electrons confined in two-dimensions [37]. We hope, therefore, that our study will stimulate further theoretical as well as experimental studies on novel ordered structures of liquid crystals and other condensed matter systems induced by such frustrations.

Acknowledgements

The work presented here is supported by the Slovenian Research Agency (ARRS research program P1-0099 and project J1-2335). J.F. is in part supported also by KAKENHI (Grant-in-Aid for Scientific Research) on Priority Area 'Soft Matter Physics' from the Ministry of Education, Culture, Sports, Science and Technology of Japan.

References

[1] Belyakov, V.A.; Dmitrienko, V.E. *Sov. Phys. Usp.* **1985**, *28*, 535–562.
[2] Stegemeyer, H.; Blümel, T.; Hiltrop, K.; Onusseit, H.; Porsch, F. *Liq. Cryst.* **1986**, *1*, 3–28.
[3] Hornreich, R.M.; Shtrikman, S. *Mol. Cryst. Liq. Cryst.* **1988**, *165*, 183–211.
[4] Dubois-Violette, E.; Pansu, B. *Mol. Cryst. Liq. Cryst.* **1988**, *165*, 151–182.
[5] Wright, D.C.; Mermin, N.D. *Rev. Mod. Phys.* **1989**, *61*, 385–432.
[6] Seideman, T. *Rep. Prog. Phys.* **1990**, *53*, 659–705.
[7] Oswald, P.; Pieranski, P. *Nematic and Cholesteric Liquid Crystals*; Taylor and Francis, 2005.
[8] Crooker, P.P. In *Chirality in Liquid Crystals*: Kitzerow, H.-S., Bahr, C., Eds.; Springer-Verlag: Berlin, 2001.
[9] Saupe, A. *Mol. Cryst. Liq. Cryst.* **1969**, *7*, 59–74.
[10] Kikuchi, H.; Yokota, M.; Hisakado, Y.; Yang, H.; Kajiyama, T. *Nat. Mater.* **2002**, *1*, 64–68.
[11] Coles, H.J.; Pivnenko, M.N. *Nature (London, UK)* **2005**, *436*, 997–1000.
[12] Cao, W.; Muñoz, A.; Palffy-Muhoray, P.; Taheri, B. *Nat. Mater.* **2002**, *1*, 111–113.
[13] Yokoyama, S.; Mashiko, S.; Kikuchi, H.; Uchida, K.; Nagamura, T. *Adv. Mater. (Weinheim, Ger.)* **2006**, *18*, 48–51.
[14] Samsung Electronics Co. Ltd., 15inch Blue Phase Mode LC Display, Seminar and Exhibition presented at the Society for Information Display (SID) 2008 International Symposium, Los Angeles, 2008.
[15] Meiboom, S.; Sethna, J.P.; Anderson, P.W.; Brinkman, W.F. *Phys. Rev. Lett.* **1981**, *46*, 1216–1219.
[16] Meiboom, S.; Sammon, M.; Brinkman, W.F. *Phys. Rev. A: At., Mol., Opt. Phys.* **1983**, *27*, 438–454.
[17] Brazovskii, S.A.; Dmitriev, S.G. *Zh. Eksp. Teor. Fiz.* **1975**, *69*, 979–989; Brazovskii, S.A.; Dmitriev, S.G. *Sov. Phys. JETP* **1976**, *42*, 497–502.
[18] Brazovskii, S.A.; Filev, V.M. *Zh. Eksp. Teor. Fiz.* **1978**, *75*, 1140–1150; Brazovskii, S.A.; Filev, V.M. *Sov. Phys. JETP* **1979**, *48*, 573–578.
[19] Dupuis, A.; Marenduzzo, D.; Yeomans, J.M. *Phys. Rev. E: Stat., Nonlinear, Soft Matter Phys.* **2005**, *71*, 011703.
[20] Alexander, G.P.; Yeomans, J.M. *Phys. Rev. E: Stat., Nonlinear, Soft Matter Phys.* **2006**, *74*, 061706.
[21] Alexander, G.P.; Marenduzzo, D. *EPL* **2008**, *81*, 66004.
[22] Alexander, G.P.; Yeomans, J.M. *Liq. Cryst.* **2009**, *36*, 1215–1227.
[23] Cates, M.E.; Henrich, O.; Marenduzzo, D.; Stratford, K. *Soft Matter* **2009**, *5*, 3791–3800.
[24] Fukuda, J.; Yoneya, M.; Yokoyama, H. *Phys. Rev. E: Stat., Nonlinear, Soft Matter Phys.* **2009**, *80*, 031706.
[25] Fukuda, J.; Žumer, S. *Phys. Rev. Lett.* **2010**, *104*, 017801.

[26] Ravnik, M.; Alexander, G.P.; Yeomans, J.M.; Žumer, S. *Faraday Discuss*. **2010**, *144*, 159–169.
[27] Crawford, G.P., Žumer, S., Eds.; *Liquid Crystals in Complex Geometries*; Taylor and Francis, 1996.
[28] Feldman, A.I.; Crooker, P.P.; Goh, L.M. *Phys. Rev. A: At., Mol., Opt. Phys*. **1987**, *35*, 842–846.
[29] Blümel, Th.; Stegemeyer, H. *Liq. Cryst*. **1988**, *3*, 195–201.
[30] Nobili, M.; Durand, G. *Phys. Rev. A: At., Mol., Opt. Phys*. **1992**, *46*, R6174–R6177.
[31] Vertogen, G.; de Jeu, W.H. *Thermotropic Liquid Crystals, Fundamentals*; Springer-Verlag: Berlin, 1988.
[32] Olmsted, P.D.; Goldbart, P.M. *Phys. Rev. A: At., Mol., Opt. Phys*. **1992**, *46*, 4966–4993.
[33] Binz, B.; Vishwanath, A.; Aji, V. *Phys. Rev. Lett*. **2006**, *96*, 207202;
[34] Rößler, U.K.; Bogdanov, A.N.; Pfleiderer, C. *Nature (London, UK)* **2006**, *442*, 797–801.
[35] Fischer, I.; Shah, N.; Rosch, A. *Phys. Rev. B: Condens. Matter Mater. Phys*. **2008**, *77*, 024415.
[36] Ho, T.L. *Phys. Rev. Lett*. **1998**, *81*, 742–745.
[37] Barrett, S.E.; Dabbagh, G.; Pfeiffer, L.N.; West, K.W.; Tycko, R. *Phys. Rev. Lett*. **1995**, *74*, 5112–5115.